

Dynamical Chaotic Inflation in the Light of BICEP2

Keisuke Harigaya,¹ Masahiro Ibe,^{1,2} Kai Schmitz,¹ and Tsutomu T. Yanagida¹

¹*Kavli IPMU (WPI), TODIAS, University of Tokyo, Kashiwa, 277-8583, Japan*

²*ICRR, University of Tokyo, Kashiwa, 277-8582, Japan*

(Dated: March 26, 2014)

The measurement of a large tensor-to-scalar ratio by the BICEP2 experiment, $r = 0.20^{+0.07}_{-0.05}$, severely restricts the landscape of viable inflationary models and shifts attention once more towards models featuring large inflaton field values. In this context, chaotic inflation based on a fractional power-law potential that is dynamically generated by the dynamics of a strongly coupled supersymmetric gauge theory appears to be particularly attractive. We revisit this class of inflation models and find that, in the light of the BICEP2 measurement, models with a non-minimal gauge group behind the dynamical model seem to be disfavored, while the model with the simplest group, i.e. $SU(2)$, is consistent with all results. We also discuss how the dynamical model can be distinguished from the standard chaotic inflation model based on a quadratic inflaton potential.

INTRODUCTION

Cosmic inflation[1] is an enormously successful paradigm of modern cosmology, which not only explains why the universe is almost homogeneous and spatially flat but which also accounts for the origin of the anisotropies in the Cosmic Microwave Background (CMB) radiation as well as for the origin of the Large Scale Structure of the Universe [2, 3]. Among the various models of inflation, chaotic inflation [4] is particularly attractive since it is free from the initial condition problem at the Planck time. Moreover, the large field values typically encountered in models of chaotic inflation predict a large contribution from gravitational waves to the CMB power spectrum [5], which can be tested by measuring the so-called B-mode of the CMB polarization spectrum. Interestingly, the BICEP2 collaboration recently announced the first measurement of just such a B-mode signal, corresponding to a tensor-to-scalar ratio of $r = 0.20^{+0.07}_{-0.05}$ at 1σ [6], which strongly suggests the presence of primordial B-mode polarization in the CMB.¹

This recent progress motivates us to revisit *dynamical chaotic inflation*, which was proposed in [8] and in which the inflaton potential is generated by the dynamics of a simple strongly coupled supersymmetric gauge theory. One prominent feature of this class of models is that it predicts a fractional power-law potential for the inflaton with the fractional power being 1 or smaller.²

Chaotic inflation of this type can be distinguished from the simplest versions of chaotic inflation, i.e. models with a quadratic or quartic potential, by precise measurements of the inflationary CMB observables. Furthermore, dynamical chaotic inflation is also attractive since it entails that the energy scale of inflation is generated via dimensional transmutation due to the strong gauge dynamics. This provides an explanation for why inflation takes place at energies much below the Planck scale.³

The organization of the paper is as follows. First, we review chaotic inflation emerging from a strongly coupled supersymmetric gauge theory, which eventually leads us to an inflaton potential proportional to some fractional power of the inflaton field. Then, we discuss how the value of the tensor-to-scalar ratio observed by BICEP2 can be explained in this class of models.

DYNAMICAL GENERATION OF THE INFLATON POTENTIAL

Let us briefly review the scenario of dynamical chaotic inflation, in which strong gauge interactions such as those proposed in [8] are responsible for the dynamical generation of the inflaton potential. For that purpose, let us consider an $SP(N)$ supersymmetric gauge theory⁴ with $2(N+2)$ chiral superfields in the fundamental representation, Q^I ($I = 1 \cdots 2(N+2)$). Besides these fundamental representations, we also introduce $(N+2)(2N+3)$ gauge-singlet chiral superfields \mathcal{Z}_{IJ} ($= -\mathcal{Z}_{JI}$), which couple to the fundamental representations in the superpotential via

$$W = \frac{1}{2} \lambda_{IJ} \mathcal{Z}_{IJ} Q^I Q^J, \quad (1)$$

¹ As pointed out in [6], the observed ratio, $r = 0.20^{+0.07}_{-0.05}$, is in tension with the upper limit on this ratio, $r < 0.11$ (at 95% C.L.) [7], which is deduced from a combination of Planck, SPT and ACT data with polarization data from WMAP. In the following discussion, we shall keep this tension in mind when applying the BICEP2 result to our dynamical model of chaotic inflation.

² Such potentials can also be realized by introducing a running kinetic term for the inflaton [9]. In string theory, fractional power-law potentials have been derived in [10]. For dynamical chaotic inflation featuring fractional powers larger than 1, cf. [11].

³ For other examples of models in which the scale of inflation is generated dynamically, cf. Refs. [12].

⁴ In our convention $SP(1)$ is equivalent to $SU(2)$. Alternative strong gauge groups, such as $SU(N)$, will be considered in [11].

with coupling constants λ_{IJ} , which we shall assume to be close to each other in the following, i.e. $\lambda_{IJ} \simeq \lambda$, for simplicity. Note that the couplings to the gauge singlets \mathcal{Z}_{IJ} in Eq. (1) lifts all of the quantum moduli, $Q^I Q^J$.

To see how the inflaton potential is generated, imagine that one of the singlet fields, $S = \mathcal{Z}_{(2N+3)(2N+4)}$ for instance, has a very large field value, so that the effective mass of $Q^{I=2N+3}$ and $Q^{J=2N+4}$ becomes much larger than the dynamical scale of the $SP(N)$ gauge interactions Λ . Then, $Q^{I=2N+3}$ and $Q^{J=2N+4}$ decouple perturbatively and the model reduces to an $SP(N)$ gauge theory with $2(N+1)$ fundamentals and $(N+1)(2N+1)$ singlets. This low energy effective theory is nothing but the dynamical supersymmetry breaking model proposed in [13]. Therefore, for a given non-vanishing S , the model breaks supersymmetry dynamically and results in a “vacuum energy” that depends on the field value of S ,

$$V \simeq \lambda^2(N+1)\Lambda_{\text{eff}}^4(S) \simeq \lambda^2(N+1)\Lambda^4 \left(\frac{\lambda|S|}{\Lambda} \right)^{\frac{2}{N+1}}. \quad (2)$$

where we have substituted the effective dynamical scale

$$\Lambda_{\text{eff}} = \Lambda \times \left(\frac{\lambda|S|}{\Lambda} \right)^{\frac{1}{2(N+1)}}, \quad (3)$$

for field values $\lambda S \gg \Lambda$.

As a result, we find that the scalar component of the singlet S obtains a fractional power-law potential,

$$V \propto |S|^p, \quad (4)$$

in which the power is solely determined by the size of the $SP(N)$ gauge group,⁵

$$p = \frac{2}{N+1}. \quad (5)$$

For example, for $SU(2) = SP(1)$, we obtain a linear potential, while a much flatter potential is generated for $N \gg 1$. In everything what follows, we will assume that the field S plays the role of the inflaton, although any of the other singlets could be equally used as well. Finally, we remark that it is easy to generalize dynamical chaotic inflation and in particular Eq. (5), such that p can also take fractional values larger than 1, cf. [11].

During chaotic inflation, the field value of the inflaton exceeds the Planck scale M_{Pl} . Before we can be sure that the above model allows for a successful implementation of chaotic inflation, we thus have to carefully examine the supergravity contributions to the scalar potential.

For example, naively coupling the above model to supergravity by simply assuming a minimal Kähler potential, $K = S^\dagger S$, leads to a very steep scalar potential

$$V \simeq e^{|S|^2/M_{\text{Pl}}^2} \times \lambda^2(N+1)\Lambda^4 \left(\frac{\lambda|S|}{\Lambda} \right)^{\frac{2}{N+1}}, \quad (6)$$

above the Planck scale. To avoid such a steep potential, we assume a shift symmetry in the direction of S [14, 15],

$$S \rightarrow S + ic, \quad c \in \mathbb{R}, \quad (7)$$

(cf. also [16] for recent developments) which renders the Kähler potential a function of $S + S^\dagger$ only,

$$K = \frac{1}{2} (S + S^\dagger)^2 + \dots, \quad (8)$$

such that it no longer depends on $\Im(S)$, the imaginary component of S . Consequently, the imaginary component of S merely has a fractional power-law potential even for $\Im(S) \gg M_{\text{Pl}}$. In the following, $\phi = \sqrt{2}\Im(S)$ is identified as the inflaton in the scenario of chaotic inflation based on the dynamically generated fractional power-law potential in Eq. (2).

It should be noted that the shift symmetry introduced in Eq. (7) is explicitly broken by the Yukawa interactions in Eq. (1), which induce the Kähler potential

$$\delta K \sim \frac{2N\lambda^2}{16\pi^2} |S|^2 \log \left(\frac{\mu^2}{M_{\text{Pl}}^2} \right), \quad (9)$$

where μ is a renormalization scale.⁶ This breaking term leads again to a steep exponential potential for $\Im(S)$ once $\Im(S) \gg M_{\text{Pl}}$. To avoid such dangerous effects, we therefore assume that λ is rather suppressed, $\lambda \ll O(10^{-1})$.⁷

TESTING DYNAMICAL CHAOTIC INFLATION

As we have demonstrated, simple strongly coupled gauge dynamics are able to generate an inflationary potential featuring a fractional power. In this section, we now outline how chaotic inflation proceeds in these models. We also summarize the predictions for the inflationary observables encoded in the CMB power spectrum.

Inflation starts out at an arbitrary initial value of the inflaton field $S = i\phi/\sqrt{2}$ above the Planck scale, $\phi \gg M_{\text{Pl}}$. There, the $SP(N)$ gauge interactions are perturbative and inflation is characterized by the slow-roll

⁵ In this letter, we only discuss the scalar potential for large field values, $\lambda S \gg \Lambda$. The vacuum structure for $\lambda S \ll \Lambda$ has been addressed in [8].

⁶ Here, we have assumed that the shift-symmetric Kähler potential in Eq. (8) is defined around the Planck scale.

⁷ Small λ is also required in order to keep the effective Q mass below the Planck scale even during inflation, $S \sim 10 \cdots 100 M_{\text{Pl}}$, i.e. $\lambda S \ll M_{\text{Pl}}$.

motion of the inflaton in the effective potential in Eq. (2) towards smaller field values. We assume that, during inflation, the strong gauge dynamics are negligible, which requires $\lambda p M_{\text{Pl}} \gg \Lambda$. Inflation finally ends once the slow-roll conditions are no longer satisfied, which happens when the inflaton field reaches $\phi \simeq p M_{\text{Pl}}$. Well after inflation, the inflaton oscillates around its origin with a mass of $m_\phi \simeq \lambda \Lambda$. At small field values, the strongly interacting theory is in the s -confinement phase [17, 18], which is well-behaved and free of singularities at the origin in field space.⁸

After inflation, the inflaton finally decays into radiation through appropriate operators. For example, the reheating temperature can be estimated as

$$T_{R,\text{dim5}} \sim 10^{12-13} \text{ GeV} \times \left(\frac{m_\phi}{10^{15} \text{ GeV}} \right)^{3/2}, \quad (10)$$

when the inflation decays into H_u and H_d Higgs fields through a dimension five operator, $K \sim (S + S^\dagger) H_u H_d$. When, instead, the inflaton decays through dimension six operators, the reheating temperature is roughly

$$T_{R,\text{dim6}} \sim 10^{8-9} \text{ GeV} \times \left(\frac{m_\phi}{10^{15} \text{ GeV}} \right)^{5/2}, \quad (11)$$

where we have assumed that the coefficients of the operators responsible for the decay of the inflation are of $O(1)$. In Eqs. (10) and (11), we have worked with an inflaton mass of $m_\phi = O(10^{15})$ GeV, which turns out to be a typical value (cf. below).⁹ As a result, we find that high reheating temperatures can be realized rather easily, which is quite favorable for successful leptogenesis [20].

Now, let us discuss the predictions of our fractional power-law inflaton potential for the CMB observables (cf. also [21]). Given the potential in Eq. (2), one finds for the power spectrum \mathcal{P}_ζ of the curvature perturbations ζ [3]

$$\mathcal{P}_\zeta = \frac{1}{6\pi^2 p^3} \left(\frac{\Lambda}{M_{\text{Pl}}} \right)^{4-p} (\lambda^2 p N_e)^{1+p/2}, \quad (12)$$

where N_e is the number of e -foldings before the end of inflation when the CMB scales leave the Hubble horizon. In Fig. 1, the red lines mark the region in the (λ, Λ) parameter space which is consistent with the observed curvature power spectrum, $\ln(10^{10} \mathcal{P}_\zeta) = 3.080 \pm 0.025$ [22]

⁸ At intermediate field values, $\lambda\phi \simeq \Lambda$, where the gauge dynamics transit from the perturbative to the strongly coupled picture, we lack the ability to precisely calculate the inflaton potential. In our discussion, we assume that the effective inflaton potential exhibits no peculiar features around Λ/λ , but that it is instead smoothly connected from one regime to the other.

⁹ Even if the mass of the inflaton is as large as 10^{15} GeV, such that its decay products have extremely large momenta, the inflaton decay products thermalize soon after their production [19].

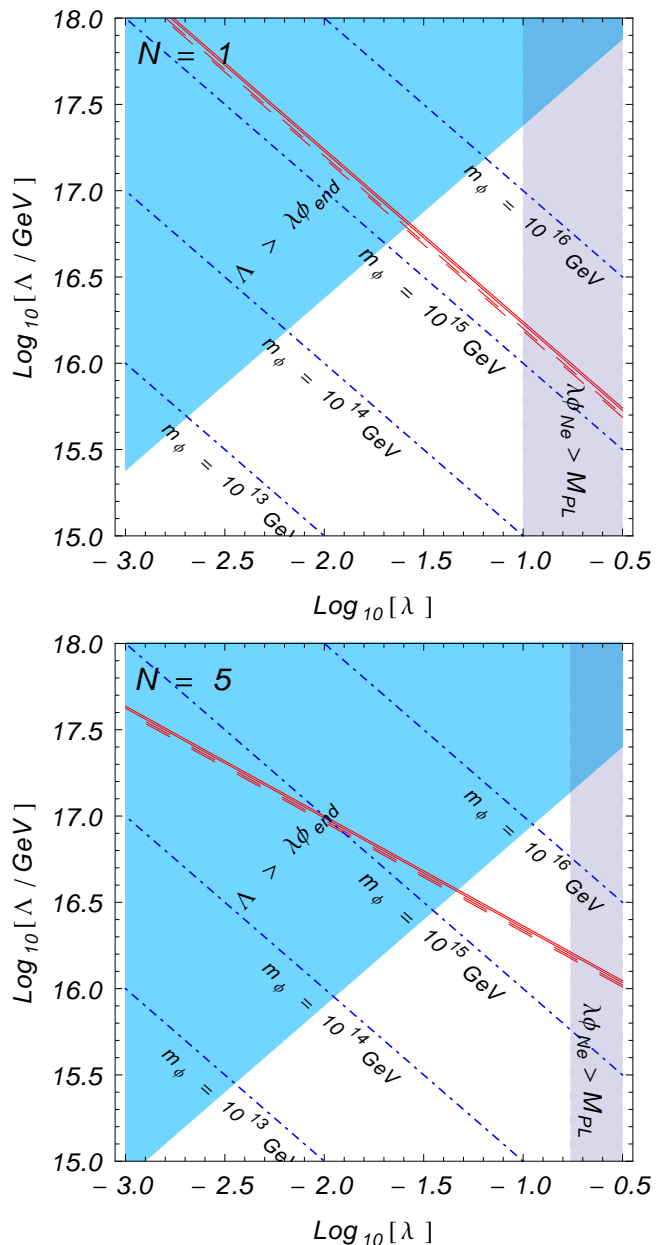


FIG. 1: (λ, Λ) plane for $N = 1$ (**upper panel**) and $N = 5$ (**lower panel**). The red lines indicate where the curvature power spectrum is consistent with the observed value within 2σ . Solid and dashed lines correspond to $N_e = 50$ and 60 , respectively. We also show contour lines for the inflaton mass as blue dot-dashed lines. The shaded regions are theoretically inaccessible because either the dynamical scale is too large, i.e. $\Lambda > \lambda\phi_{\text{end}}$, or the coupling constant λ is too large, i.e. $\lambda\phi_{N_e} > M_{\text{Pl}}$, as denoted in the figure.

for $N = 1$ and $N = 5$, respectively. The blue dot-dashed lines represent contour lines indicating the values of the inflaton mass. In the blue-shaded regions, the dynamical scale is rather large, so that is also important during inflation, i.e. $\Lambda > \lambda\phi_{\text{end}}$, where $\phi_{\text{end}} \simeq p M_{\text{Pl}}$. In this situation, we loose control over the inflaton potential, as

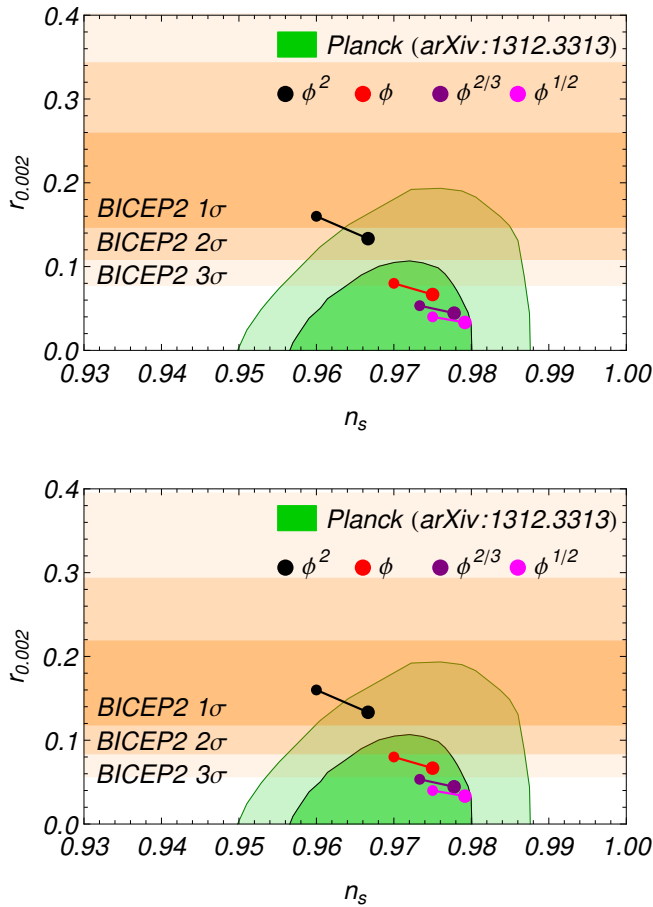


FIG. 2: Predicted values for n_s and r for $p = 1$ ($N = 1$), $p = 2/3$ ($N = 2$), and $p = 1/2$ ($N = 3$). Here, $r_{0.002}$ denotes the tensor-to-scalar ratio at the pivot scale $k = 0.002 \text{ Mpc}^{-1}$. The predictions according to chaotic inflation with a quadratic potential are also shown for comparison. Small and big dots stand for $N_e = 50$ and 60 , respectively. The green contours are the constraints extracted from [22]. The orange bands correspond to the 1 , 2 and 3σ ranges for r measured by BICEP2. Here, the bands in the **upper panel** are purely based on the BICEP2 maps, while the bands in the **lower panel** follow after subtracting the cross correlation spectrum for the DDM2 foreground polarization model [6] from the raw data.

it becomes distorted by incalculable strong coupling effects. On the other hand, in the gray-shaded regions, the coupling λ is too large, such that the effective mass of the heavy Q 's exceeds M_{Pl} during inflation, i.e. $\lambda\phi_{N_e} > M_{\text{Pl}}$ with $\phi_{N_e} \simeq (2pN_e)^{1/2} M_{\text{Pl}}$. In conclusion, Fig.1 illustrates that the observed curvature power spectrum can be reproduced for $\lambda \simeq 10^{-(2-1)}$ and $\Lambda \simeq 10^{16} \text{ GeV}$, where the inflaton mass is typically of $O(10^{15}) \text{ GeV}$.

The spectral index n_s , the running of the spectral index $dn_s/d\ln k$, and the tensor-to-scalar ratio r of the

curvature perturbations are predicted to be,

$$n_s = 1 - \frac{p+2}{2N_e}, \quad \frac{dn_s}{d\ln k} = -\frac{2+p}{2N_e^2}, \quad r = \frac{4p}{N_e}. \quad (13)$$

In the two panels of Fig. 2, we show the predicted values for n_s and r for $p = 1$ ($N = 1$), $p = 2/3$ ($N = 2$), and $p = 1/2$ ($N = 3$). At the same time, dynamical chaotic inflation predicts the running of the spectral index to be negligibly small. In Fig. 2, we also reproduce the constraints on n_s and r presented in [22], in which the Planck data has been re-analyzed taking particular care of possible systematics in the 217 GHz temperature map. Furthermore, we include constraints on the tensor-to-scalar ratio as deduced from the BICEP2 measurement. In the upper panel of Fig. 2, we indicate the r value derived from the pure BICEP2 signal, $r = 0.20^{+0.07}_{-0.05}$, while in the lower panel of this figure, we display the allowed r range obtained by the BICEP2 collaboration after subtracting the arguably best model for foreground dust polarization from the raw data, $r = 0.16^{+0.06}_{-0.05}$. In summary, this figure shows that models with $N > 1$ are excluded by the BICEP2 results at the 3σ level. By contrast, the simplest case, i.e. $N = 1$, is consistent with the BICEP2 result within 3σ . In fact, for $N = 1$ and $N_e = 50$, dynamical chaotic inflation predicts $r \simeq 0.08$, which deviates from the BICEP2 maximum likelihood value, $r = 0.20$, by 2.9σ as well as from the corresponding value after subtraction of the DDM2 dust foreground model, $r = 0.16$, by 2.1σ . A complete comparison of our prediction for r in the simplest case of an $SU(2)$ gauge group with the allowed r ranges obtained for all of the various foreground models considered by the BICEP2 collaboration can be found in Fig 3. More general scenarios of dynamical chaotic inflation, also featuring fractional powers $p > 1$, as well as their performance in view of the BICEP2 results will be addressed in [11].

In view of the above stated deviations between our prediction of $r \simeq 0.08$ and the experimental values, it is important to note that at present there is a tension between the constraints deduced from the Planck data and the value measured by BICEP2, where the Planck data favors a smaller value of the tensor-to-scalar ratio. Moreover, as far as our theoretical prediction is concerned, we also remark that, if the shift symmetry is broken not only in the superpotential but also in the Kähler potential, the prediction for r can be still be raised to larger values [16, 23–25]. The same applies to generalized dynamical chaotic inflation featuring fractional powers $p > 1$ [11]. Therefore, it is certainly premature to declare dynamical chaotic inflation ruled out by the data at this point, in particular, the model with the simplest gauge group $SU(2)$. Quite the contrary, as further measurements of the CMB B-mode polarization are being performed, dynamical chaotic inflation based on strong $SU(2)$ dynamics might eventually develop into one of the most promising models correctly describing the data.

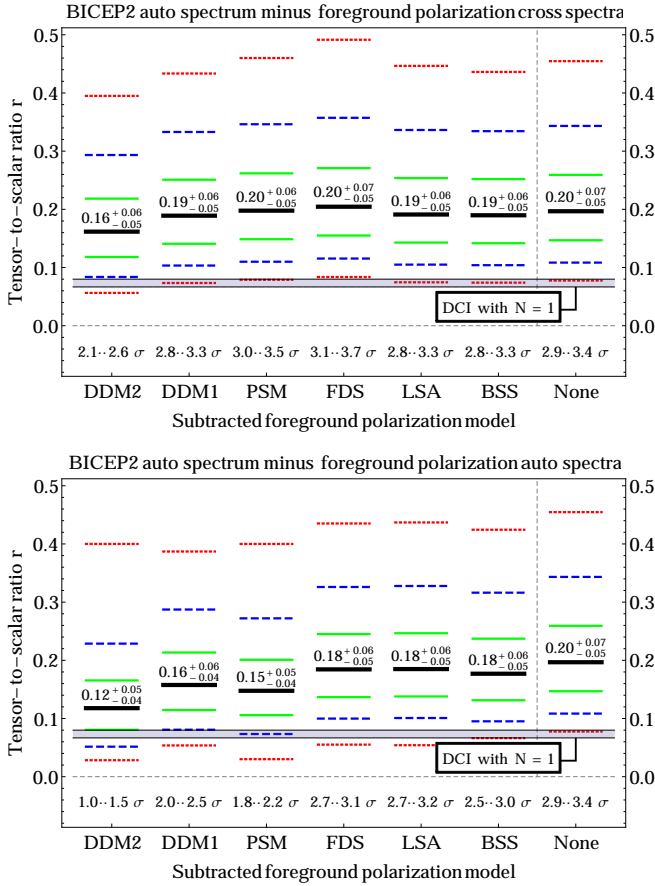


FIG. 3: Comparison between our prediction for r in the case of dynamical chaotic inflation (DCI) based on $SU(2)$ gauge dynamics, $r = 4/N_e \simeq 0.07 \cdots 0.08$, (gray band) and the maximum likelihood values for r deduced from the BICEP2 measurement and various foreground polarization models [6]. The **upper** and the **lower panel** are respectively based on the subtraction of the cross and auto spectra from the raw data. For each model and subtraction procedure, we state the maximum likelihood value for r , its 1σ range as well as the deviation of our prediction from this value. Here, the uncertainty in the latter figure stems from the uncertainty in N_e . In addition to that, the colorful bars mark the respective 1σ (solid, green), 2σ (dashed, blue) and 3σ (dotted, red) ranges for r .

Another important key feature of dynamical chaotic inflation is that it predicts a slightly larger value for the spectral index compared with the simplest chaotic inflation model. Therefore, by further observational investigation of n_s and r , dynamical chaotic inflation can be distinguished from the simplest model of chaotic inflation based on a quadratic potential.¹⁰

¹⁰ Fig. 2 slightly suggests that a smaller number of e -foldings N_e (lower T_R) is preferred in the case of the dynamical model, so

CONCLUSIONS

In this paper, we revisited the class of models of chaotic inflation the potential of which is generated by the dynamics of a strongly coupled supersymmetric gauge theory. A prominent feature of this scenario of *dynamical chaotic inflation* is that the inflaton potential features a fractional power. Contrasting dynamical chaotic inflation with the tensor-to-scalar ratio recently observed by the BICEP2 experiment, we find that models with non-minimal gauge group seem to be disfavored, while the model based on the simplest gauge group, $SU(2)$, is barely consistent with observations. However, since there is a tension between the Planck constraints and the BICEP2 measurement, we need to wait for further confirmation/refutation by other observations such as Planck, ACTpole, SPT, and POLARBEAR. Only with additional data at hand, it will become clear whether dynamical chaotic inflation is excluded or in fact a good description of the CMB data. Likewise, improved constraints on n_s will also help to distinguish the dynamical chaotic inflation model from chaotic inflation based on a quadratic potential.

Acknowledgements This work is supported by Grant-in-Aid for Scientific Research from the Ministry of Education, Science, Sports, and Culture (MEXT), Japan, No. 22244021 (T.T.Y.), No. 24740151 (M.I.), and by the World Premier International Research Center Initiative, MEXT, Japan. The work of K.H. is supported in part by a JSPS Research Fellowship for Young Scientists.

- [1] A. H. Guth, Phys. Rev. D **23**, 347 (1981); A. D. Linde, Phys. Lett. B **108**, 389 (1982); A. Albrecht and P. J. Steinhardt, Phys. Rev. Lett. **48**, 1220 (1982).
- [2] V. F. Mukhanov and G. V. Chibisov, JETP Lett. **33**, 532 (1981) [Pisma Zh. Eksp. Teor. Fiz. **33**, 549 (1981)]; A. D. Linde, Contemp. Concepts Phys. **5**, 1 (1990) [hep-th/0503203].
- [3] D. H. Lyth and A. Riotto, Phys. Rept. **314**, 1 (1999) [hep-ph/9807278].
- [4] A. D. Linde, Phys. Lett. B **129**, 177 (1983); A. D. Linde, JETP Lett. **38**, 176 (1983) [Pisma Zh. Eksp. Teor. Fiz. **38**, 149 (1983)].
- [5] A. A. Starobinsky, Sov. Astron. Lett. **11**, 133 (1985); D. H. Lyth, Phys. Rev. Lett. **78**, 1861 (1997) [hep-ph/9606387].
- [6] P. A. R. Ade *et al.* [BICEP2 Collaboration], arXiv:1403.3985 [astro-ph.CO].

as to raise the tensor-to-scalar ratio towards the BICEP2 best-fit value, while a larger number of e -foldings N_e (higher T_R) is preferred in the case of the quadratic potential model, so as to make the spectral index larger.

- [7] P. A. R. Ade *et al.* [Planck Collaboration], arXiv:1303.5076 [astro-ph.CO].
- [8] K. Harigaya, M. Ibe, K. Schmitz and T. T. Yanagida, Phys. Lett. B **720**, 125 (2013) [arXiv:1211.6241 [hep-ph]].
- [9] F. Takahashi, Phys. Lett. B **693**, 140 (2010) [arXiv:1006.2801 [hep-ph]].
- [10] E. Silverstein and A. Westphal, Phys. Rev. D **78**, 106003 (2008) [arXiv:0803.3085 [hep-th]].
- [11] K. Harigaya, M. Ibe, K. Schmitz and T. T. Yanagida, In preparation.
- [12] S. Dimopoulos, G. R. Dvali and R. Rattazzi, Phys. Lett. B **410**, 119 (1997) [hep-ph/9705348]; K. I. Izawa, M. Kawasaki and T. Yanagida, Phys. Lett. B **411**, 249 (1997) [hep-ph/9707201]; K. I. Izawa, Prog. Theor. Phys. **99**, 157 (1998) [hep-ph/9708315].
- [13] K. -I. Izawa and T. Yanagida, Prog. Theor. Phys. **95**, 829 (1996) [hep-th/9602180]; K. A. Intriligator and S. D. Thomas, Nucl. Phys. B **473**, 121 (1996) [hep-th/9603158].
- [14] M. Kawasaki, M. Yamaguchi and T. Yanagida, Phys. Rev. Lett. **85**, 3572 (2000) [hep-ph/0004243].
- [15] R. Kallosh, A. Linde, K. A. Olive and T. Rube, Phys. Rev. D **84**, 083519 (2011) [arXiv:1106.6025 [hep-th]]; For a recent review, see also A. Linde, arXiv:1402.0526 [hep-th].
- [16] R. Kallosh and A. Linde, JCAP **1011**, 011 (2010) [arXiv:1008.3375 [hep-th]].
- [17] N. Seiberg, Phys. Rev. D **49**, 6857 (1994) [hep-th/9402044];
- [18] K. A. Intriligator and P. Pouliot, Phys. Lett. B **353**, 471 (1995) [hep-th/9505006]; C. Csaki, M. Schmaltz and W. Skiba, Phys. Rev. Lett. **78**, 799 (1997) [hep-th/9610139].
- [19] K. Harigaya and K. Mukaida, arXiv:1312.3097 [hep-ph].
- [20] M. Fukugita and T. Yanagida, Phys. Lett. B **174** (1986) 45.
- [21] L. Alabidi and I. Huston, JCAP **1008**, 037 (2010) [arXiv:1004.4794 [astro-ph.CO]]; J. Martin, C. Ringeval and R. Trotta, Phys. Rev. D **83**, 063524 (2011) [arXiv:1009.4157 [astro-ph.CO]].
- [22] D. Spergel, R. Flauger and R. Hlozek, arXiv:1312.3313 [astro-ph.CO].
- [23] R. Kallosh, A. Linde and T. Rube, Phys. Rev. D **83**, 043507 (2011) [arXiv:1011.5945 [hep-th]].
- [24] T. Li, Z. Li and D. V. Nanopoulos, JCAP **1402**, 028 (2014) [arXiv:1311.6770 [hep-ph]].
- [25] K. Harigaya and T. T. Yanagida, arXiv:1403.4729 [hep-ph].